PLOS Water

RESEARCH ARTICLE

Ongoing mercury contamination downstream from the former New Idria Mercury Mine: Southern diablo range of the California coast ranges

Rachel A. Hohn[1]*, Khalil P. Abusaba[2,3], Erin N. Bray[4], Scott C. Hauswirth[1], Byran C. Fuhrmann[5,6], Marc W. Beutel[6], Carl H. Lamborg[2], Robert P. Mason[7], Aurthur R. Flegal[2], Priya M. Ganguli[1,2]

1 California State University, Northridge, California, United States of America, **2** University of California, Santa Cruz, California, United States of America, **3** Brown and Caldwell, Walnut Creek, California, United States of America, **4** San Francisco State University, San Francisco, California, United States of America, **5** SePRO Corporation, Whitakers, North Carolina, United States of America, **6** University of California, Merced, California, United States of America, **7** University of Connecticut, Groton, Connecticut, United States of America

* rhohn.csun@gmail.com

OPEN ACCESS

Citation: Hohn RA, Abusaba KP, Bray EN, Hauswirth SC, Fuhrmann BC, Beutel MW, et al. (2025) Ongoing mercury contamination downstream from the former New Idria Mercury Mine: Southern diablo range of the California coast ranges. PLOS Water 4(6): e0000328. https://doi.org/10.1371/journal.pwat.0000328

Editor: Inderjeet Tyagi, ZSI: Zoological Survey of India, INDIA

Received: January 2, 2024

Accepted: December 2, 2024

Published: June 6, 2025

Peer Review History: PLOS recognizes the benefits of transparency in the peer review process; therefore, we enable the publication of all of the content of peer review and author responses alongside final, published articles. The editorial history of this article is available here: https://doi.org/10.1371/journal.pwat.0000328

Abstract

California's mining legacy continues to threaten water quality and ecosystem health throughout the state. This study focuses on mercury (Hg) releases from the former New Idria Mercury Mine, which was the second largest historic Hg producer in North America. San Carlos Creek, which flows adjacent to the mine, is impacted by acid mine drainage (AMD) as well as mining waste piles that sit at a high angle of repose over the channel. We documented total mercury (HgT) concentrations exceeding California's 50 ng L^{-1} water quality objective for almost 10 km, from New Idria to a ~ 0.25 km^2 perennial wetland at the confluence of San Carlos Creek and Silver Creek within the Panoche Creek watershed. During baseflow and low flow storm conditions, unfiltered total Hg (U-HgT) in creek water downstream from the mine typically ranged from 1,100–9,200 ng Hg L^{-1}, with >90% of Hg in the particulate phase. U-HgT correlated ($R^2 = 0.6$) with suspended particulate matter (SPM) that was presumably a mixture of AMD-derived flocculant, weathered calcines (i.e., roasted ore), and sediment from the local watershed. The flocculant is easily resuspended in baseflow conditions and scoured from the channel during high flow events, resulting in seasonal patterns of Hg transport in San Carlos Creek that do not always align with the stream hydrograph. Mercury from New Idria, along with AMD flocculant, metals, sulfate, and other anions, presumably accumulate or infiltrate at the Silver Creek wetland until larger storms remobilize sediments further downstream towards the ~ 0.65 km^2 Panoche Creek Wetland, the Panoche Fan, and ultimately to the Fresno Slough, Mendota Wildlife Area, Mendota Pool and San Joaquin River.

Data availability statement: All data reported in this manuscript are available in S1 and S2 Tables, which are being published with this manuscript as Supporting Information.

Funding: Field work and laboratory analyses associated with with this project were supported by a grant from the California State University (CSU) Water Resources and Policy Initiative Affinity Group (WRPI, now CSU WATER) awarded to PMG and by start up funding provided by CSU Northridge's (CSUN) College of Math and Science (PMG) and College of Social and Behavioral Sciences (ENB). Graduate student support for RAH was provided by the Geological Society of America (GSA) and from CSUN's Office of Graduate Studies, Association of Retired Faculty, and Department of Geological Sciences Hanna Fellowship Program. CSU-WATER: https://www.calstate.edu/impact-of-the-csu/research/water CSUN College of Math and Science: https://w2.csun.edu/science-mathematics/college CSUN College of Social and Behavioral Sciences: https://www.csun.edu/social-behavioral-sciences Geological Society of America (GSA): https://www.geosociety.org/GSA/GSA/grants/gradgrants.aspx CSUN Office of Graduate Studies: https://www.csun.edu/graduate-studies/student-funding CSUN Association of Retired Faculty: https://www.csun.edu/arf/scholarships.html CSUN Department of Geological Sciences: https://www.csun.edu/science-mathematics/geology

Competing interests: The authors have declared that no competing interests exist.

1. Introduction

1.1. Mining and other mercury sources

The majority of mercury (Hg) in the modern environment is associated with human activities that have taken place over the past 500 years [1]. Elemental Hg (Hg^0), the familiar "quicksilver" which is a liquid at room temperature, amalgamates readily with gold. As a result, artisanal and small-scale gold mining operations are one of the largest sources of Hg contamination [2]. Mercury's affinity for organic carbon makes coal combustion another primary source of anthropogenic Hg [3,4]. Historically, Hg was also used as a primer for military ammunition, and later in long-life mercuric oxide batteries [5]. Although ore from New Idria initially provided quicksilver for gold and silver mining, it later supplied strategic national Hg reserves needed to fight the Korean War and the Vietnam War [6]. Mercury is still an important industrial catalyst in processes such as manufacturing caustic soda [7]. The United States signed the Minamata Convention on Mercury in 2013. This convention aims to protect human health and the environment by limiting mercury emissions from various sources, including mining, manufacturing, and waste disposal, with a specific emphasis on phasing out mercury use in products and processes like the chlor-alkali production [8].

In California, where coal combustion is minimal, legacy Hg and gold mines are the primary within-state source of Hg contamination to aquatic ecosystems [9,10]. Mercury contaminated watersheds exists throughout the Sierra Nevada Mountains due to gold mining [11,12] and throughout the California Coast Ranges due to Hg mining [Fig 1; 13–15] [Fig. In fact, the two largest historic Hg mines in North America – New Almaden and New Idria – are located in California. Jew et al. [16] measured gaseous elemental mercury (GEM) evasion from lab-tested waste rock from New Idria, New Almaden, and other California Coast Range Hg mines, indicating legacy mining continues to degrade air quality, in addition to water quality.

Numerous studies document Hg transport from New Almaden as well as downstream ecosystem impacts [17–19]. Mercury isotopes in San Francisco Bay show that contamination from New Almaden increases the concentration of Hg in South San Francisco Bay sediments [20] and forage fish [21]. At New Idria, substantial applied research has been conducted on Hg in solid mining waste [16,22–27]. However, only one peer-reviewed study has confirmed Hg uptake by local vegetation [28], and the only study to document aquatic Hg transport was conducted in the late 1990s [13], prior to on-site remedial actions completed in 2012 and 2015. The data and geochemical evaluations in this paper confirm the prior studies and demonstrate ongoing release of acid mine drainage (AMD) and Hg from New Idria towards biologically important habitats within the San Joaquin River Watershed. To our knowledge, no published data exists on downstream ecosystem impacts from the site, such as food web transfer to primary consumers or predators.

1.2. Mercury biogeochemistry

Mercury occurs naturally in the environment and does not degrade. It does, however, transform between inorganic, elemental, and organic chemical species [Fig 2; 29].

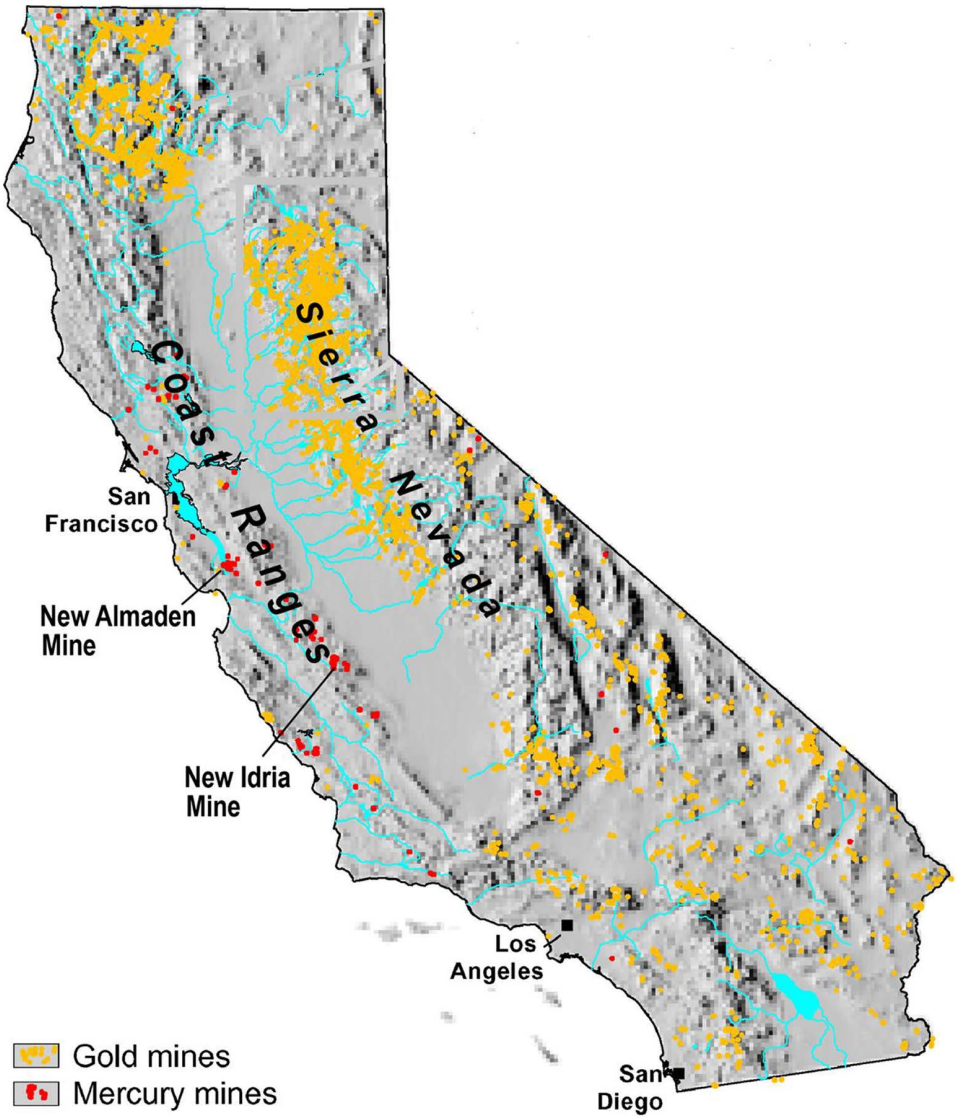

Fig 1. Locations of historic gold and mercury mines in California. New Almaden and New Idria were the largest mercury producers in North America. After Alpers, et al., 2005 [11].

https://doi.org/10.1371/journal.pwat.0000328.g001

Combustion-sources of Hg, such as mining and burning fossil fuels, have drastically increased atmospheric Hg concentrations [30]. This Hg occurs predominantly as GEM in the atmosphere with a lesser amount present as gaseous oxidized mercury (GOM) [31]. Although reactive gaseous mercury (GOM plus particulate airborne mercury) deposits from the atmosphere in hours to days, GEM has an atmospheric residence time of less than a year before oxidation and deposition as GOM [32], similar to the atmospheric mixing time of Earth's hemispheres [33]. Thus, once in the atmosphere, GEM disperses globally, reaching remote locations that have no direct Hg source [34,35]. The most abundant form of Hg in terrestrial ecosystems is inorganic divalent Hg (Hg^{2+}), which is also the form present in Hg sulfide ores, including cinnabar and metacinnabar [HgS; 36,37].

Although inorganic Hg(II) and Hg^0 are the primary chemical species associated with anthropogenic activities, organic monomethylmercury (CH_3Hg^+ or MeHg) is the form that poses the greatest threat to humans and wildlife because it

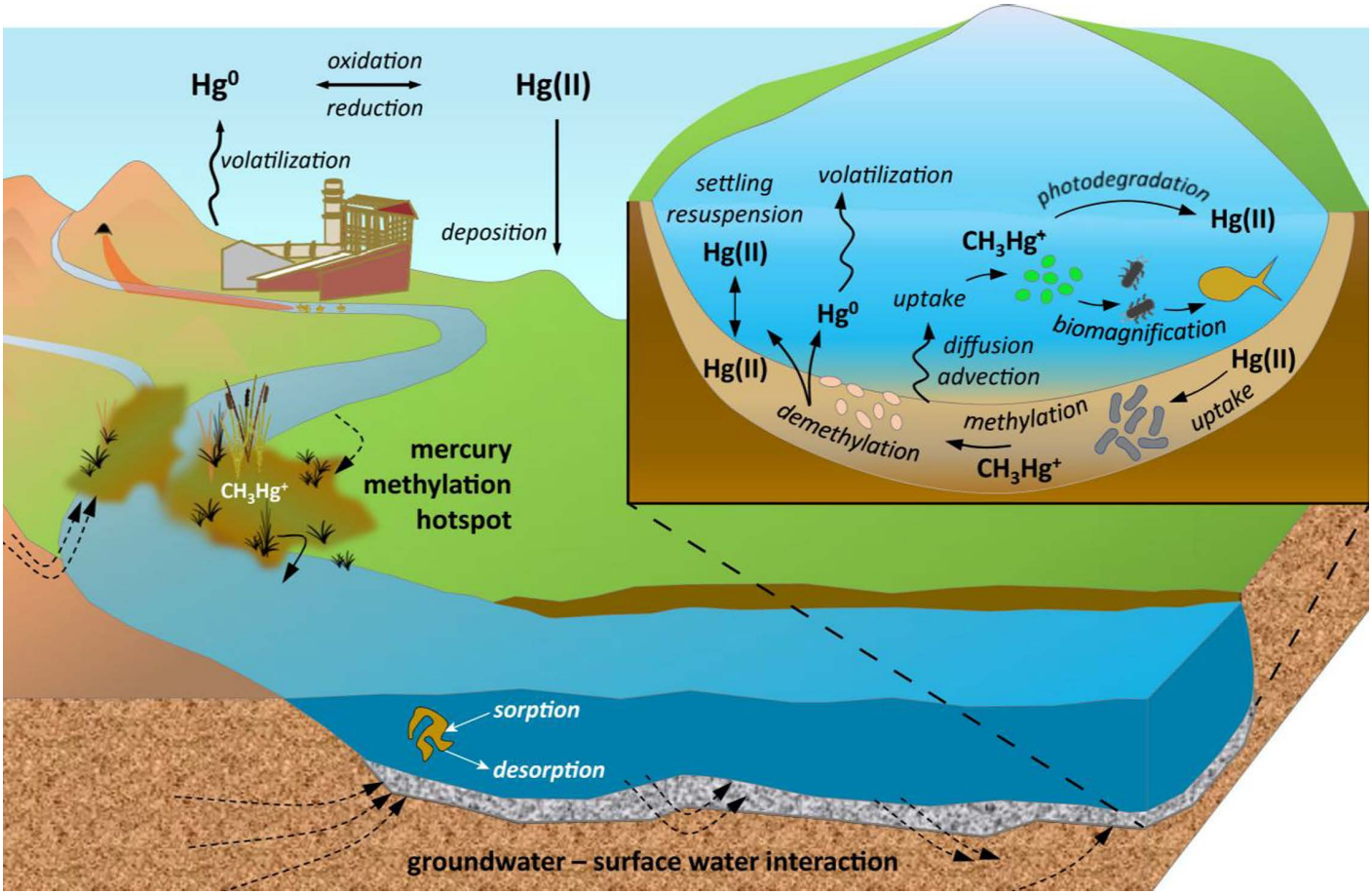

Fig 2. Illustration highlighting some of the physical and biological processes that influence Hg biogeochemical cycling in stream environments.

https://doi.org/10.1371/journal.pwat.0000328.g002

bioaccumulates in individual organisms and then biomagnifies as it is transferred to higher trophic levels in the food web [38; Fig 2]. In fact, MeHg biomagnifies so efficiently that apex predators can have >10^6 times more MeHg their tissue relative to the water in their habitat [30,39,40] and the primary way humans are exposed to Hg is by consuming fish [4;41]. The neurotoxicity of MeHg is particularly concerning because this molecule can pass the blood-brain barrier and the placenta wall, impairing the central nervous system which controls abilities such as motor skills and cognition [42]. Growing fetuses and the young offspring of humans and wildlife are, therefore, at the greatest risk of impairment [43].

MeHg in contaminated terrestrial and coastal systems is primarily formed biotically by anaerobic bacteria, often sulfate-reducing bacteria [7,44,45]. This makes habitats that have abundant low oxygen zones and complex food webs particularly conducive to Hg methylation and biomagnification [46]. Organic carbon metabolism can promote anaerobic conditions that stimulate methylating bacteria, but organic carbon with abundant thiol groups can reduce the availability of Hg to methylating bacteria [47]. Once formed, MeHg can be broken down abiotically photosynthetically active radiation in coastal and inland waters [48]. Biotic degradation of MeHg by demethylating bacteria is also an important loss pathway, particularly in contaminated systems [49; Fig 2]. Therefore, the concentration of MeHg in a system depends on the rates of microbial methylation as well as abiotic and biotic demethylation, which converts MeHg into either Hg^{2+} or Hg^0 [49].

Marvin-DiPasquale et al. [49] showed that at New Idria, microbial demethylation occurs by the latter pathway (generation of Hg^0), which is thought to be a detoxification mechanism common to highly contaminated ecosystems.

2. Study site

2.1. Hydrologic setting and mining history

New Idria is an abandoned mine town in the Diablo Range of the California Coast Ranges in San Benito County, California (Fig 3). This region has a Mediterranean climate, with little to no rain in the summer months. San Carlos Creek, which receives discharge from New Idria, is located within the Panoche Creek watershed and the nearest United States Geological Survey (USGS) streamflow gaging station is on Panoche Creek (11255575) about 40 km downstream from the mine. Over the duration of this ~450-day study (Jan 2019 – Mar 2020), the Panoche Creek gage registered flow on 181 days,

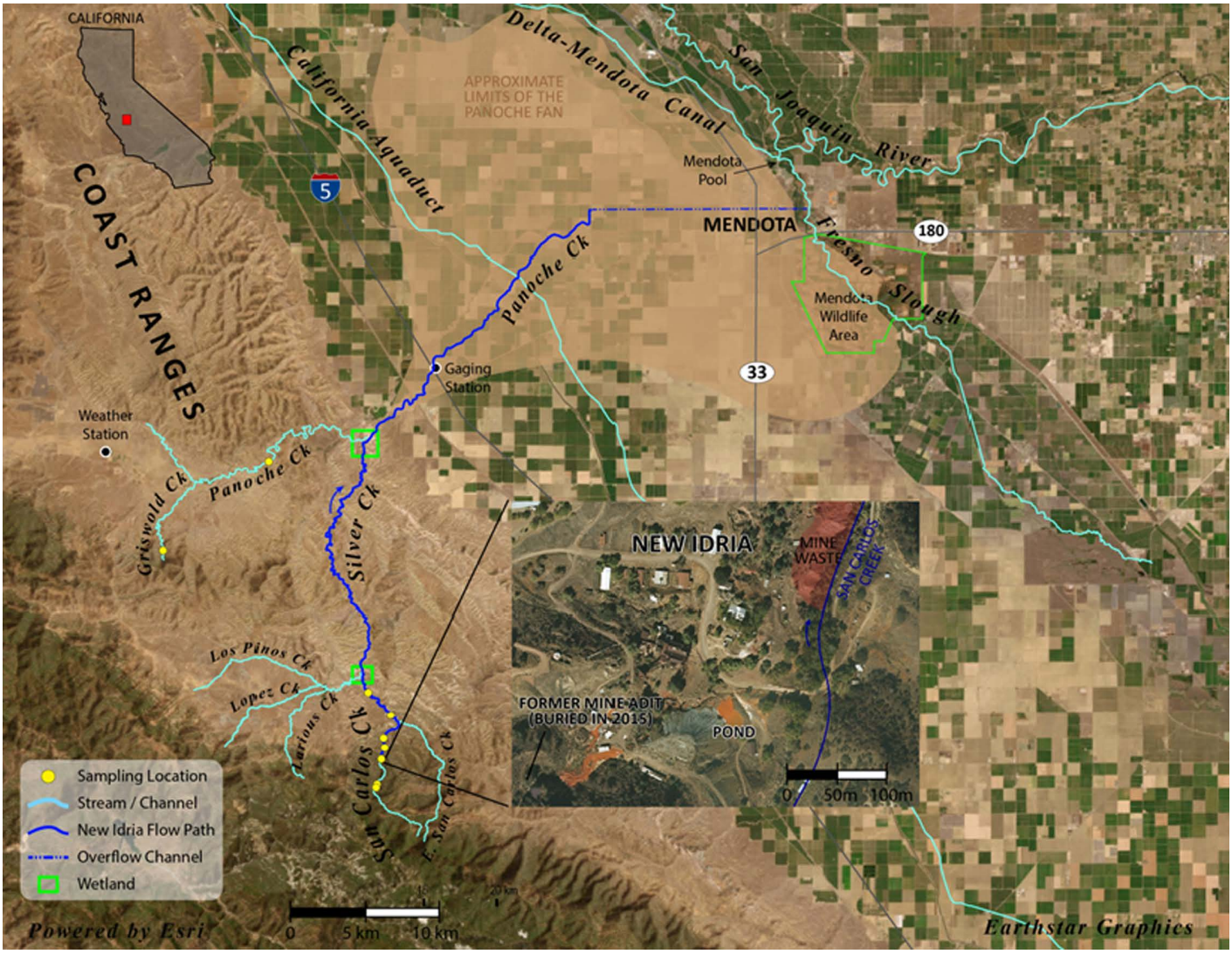

Fig 3. Regional map of the study area showing sampling locations, the flow path from New Idria to the Fresno Slough in Mendota, CA, and the approximate extent of the Panoche Creek Fan [50].

https://doi.org/10.1371/journal.pwat.0000328.g003

with an average discharge of 0.13 $m^3 s^{-1}$ and a maximum discharge of 2.5 $m^3 s^{-1}$. The infrequency of substantial flow at the gaging station compared to annual precipitation (S1 Fig) underscores the transient nature of the surface water hydrologic connection from New Idria to downstream ecosystems of the Mendota Wildlife Area and the Mendota Pool.

The New Idria Mining District includes the New Idria Mine along with over a dozen smaller mines. It was operational for about 115 years (~1854 – 1972) and produced more than 2.0 x 10^7 kg of Hg, making it the second largest Hg mine in North America [51,52]. Cinnabar and metacinnabar along with iron-bearing low-value gangue minerals were deposited in fractures by low-temperature hydrothermal fluids [26,53]. The ore occurs in veins of silica-carbonate rock along the margins of Panoche shales and a domed serpentinite formation [53,54]. Serpentinite, which is the state rock of California, increases the natural background concentrations of chromium, nickel and asbestos in water and soils upstream of New Idria [52,55]. New Idria's unique geologic setting also makes it one of the only locations in the world where benitoite, the state gem of California, can be found [56].

The Level 10 Adit (adit) marks the exit of the horizontal tunnel used to bring cinnabar extracted from a network of smaller mining tunnels to the furnace roasting facilities (Fig 4). Groundwater and surface water infiltration has flooded the interconnected mine tunnels [57], putting water in contact with pyrite (FeS) and marcasite (FeS_2). These iron-rich minerals react with water and oxygen to form AMD via a series of microbial and chemical processes [58].

Prior to 2015, AMD spread across the site before entering an 810 m^2 (0.2-acre) settling pond that overflows into San Carlos Creek, a small mountain stream that skirts the eastern margin of the mine (Fig 4). The stream typically turns orange, and sometimes white, as AMD enters the channel, and then travels about 0.5 km along the toe of mining waste piles that cover over 0.16 km^2 (40 acres) of land [57; Fig 4 and S2 Fig]. Measurements made in the late 1990s found that AMD accounted for almost half the stream flow in San Carlos Creek downstream from New Idria. Dry season discharge increased from 3 to 5 L s^{-1} after AMD entered the channel and wet season discharge increased from 13 to 24 L s^{-1} [13]. Subsurface AMD flow near the pond was also inferred in a geophysical investigation conducted by the US Environmental Agency (EPA) in 2012 [57].

2.2. Downstream ecosystems

About 10 km north of the mine, a 0.25 km^2 (60-acre) perennial riparian wetland forms where San Carlos and Larious Creeks join to become Silver Creek (Fig 3). The Silver Creek wetland is supplied by continuous flow from San Carlos Creek, ephemeral flow from Larious Creek, and potentially by groundwater inputs from the Vallecitos Valley groundwater basin (S3 Fig). The relative contribution from each source is unknown. Vallecitos Valley groundwater and surface water are naturally high in salt content from Tertiary age marine sediments [50], contributing to elevated levels of selenium in the groundwater and sediments of this region [59].

A second 0.65 km^2 (160-acre) perennial riparian wetland forms about 35 km downstream from New Idria, where Silver Creek joins Panoche Creek (Fig 3). After exiting the wetland, Panoche Creek flows eastward towards the San Joaquin Valley and, during most years, terminates within the Panoche Creek alluvial fan (Panoche Fan). During moderate to heavy precipitation events, Panoche Creek flows beyond the Panoche Fan along Route J1 (Belmont Avenue) before discharging into the Fresno Slough about 5 km upstream from the San Joaquin River, near the Mendota Wildlife Area. This flow path creates an intermittent hydrologic connection between the New Idria Mine and the San Joaquin River [60].

2.3. Regulatory setting

San Carlos Creek is listed as impaired for Hg under the Clean Water Act Section 303(d) list [61]. The New Idria Mine Superfund site (site) was added to EPA's National Priorities List in 2011 and a potentially responsible party (PRP) was identified. In 2012 the EPA conducted emergency remedial actions to reduce contaminant releases from the site [62]. These actions included: sealing the Level 10 Adit's surface discharge and re-routing AMD through subsurface piping to

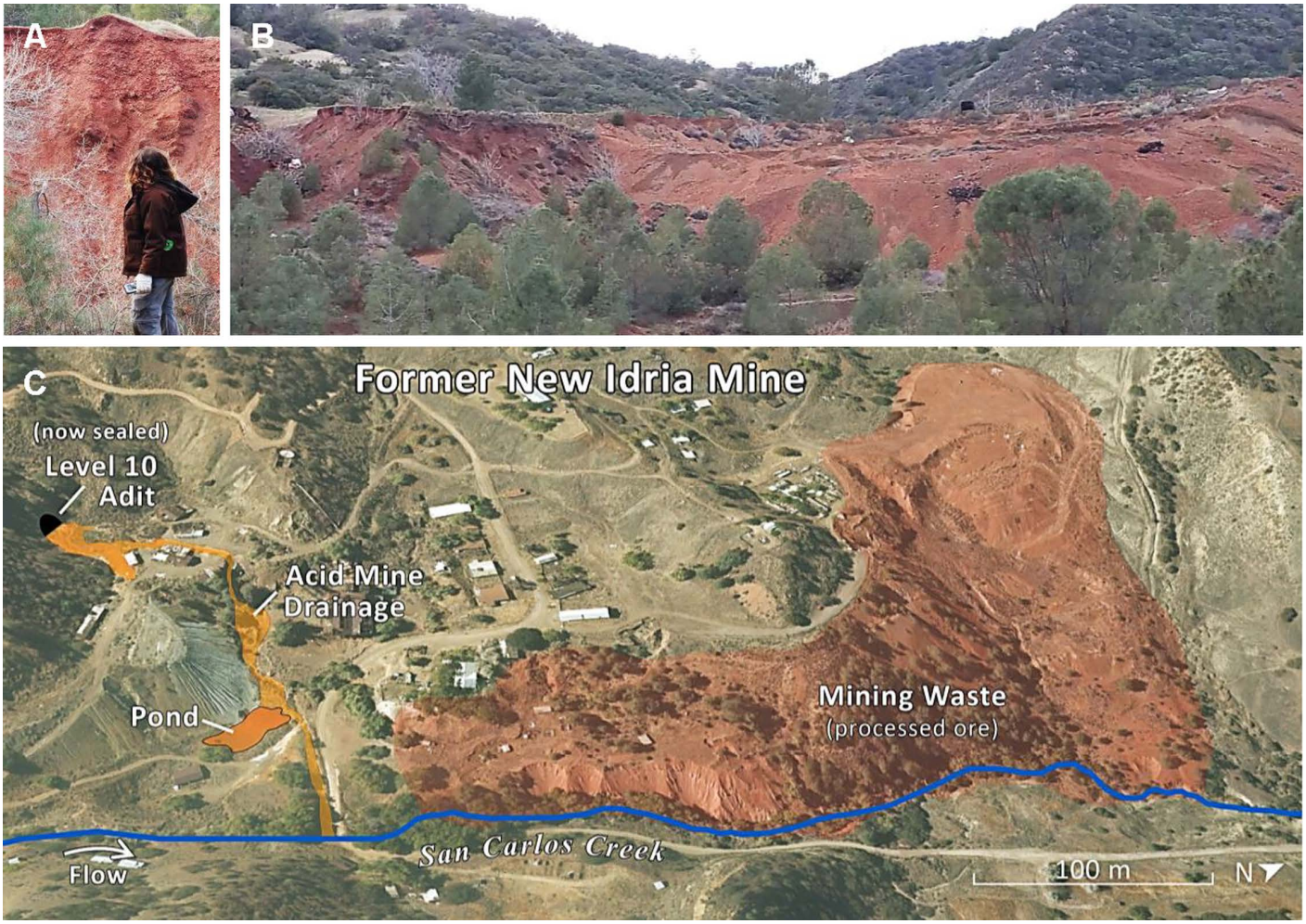

Fig 4. (A) Vertical wall of exposed mining waste along the channel of San Carlos Creek. (B) Profile view of waste piles with riparian vegetation in the foreground. (C) Oblique view of the former New Idria Mine showing AMD exiting the Level 10 Adit prior to EPA's remedial actions and the approximate extent of the solid waste piles.

https://doi.org/10.1371/journal.pwat.0000328.g004

reduce its contact with mining waste; expanding the settling pond to increase detention time; constructing surface water diversions to direct runoff away from waste; and improving site security. In 2015, the PRP stabilized a tailings pile around a potable water pipeline serving local residents and dredged the pond to further increase its capacity. Despite capacity expansions, the relatively small pond continuously discharges AMD. The PRP and EPA agreed to a settlement in 2018 [62] committing the PRP to perform a remedial investigation and feasibility study (RI/FS) in accordance with EPA guidance under the Comprehensive Environmental Response, Compensation, and Liability Act (CERCLA). EPA makes technical and legacy documents, fact sheets, and updates related to New Idria publicly available through its Superfund website [63].

Since fish consumption is the primary Hg exposure route for humans, EPA established a water quality standard for MeHg in an effort to control Hg concentrations in fish [64]. EPA subsequently issued guidance [TMDLs;] translating these fish-tissue based targets into state water quality regulatory plans regulating THg, such as wastewater discharge permits and watershed pollutant reduction plans referred to as Total Maximum Daily Loads (TMDLs). New Idria is in the San Joaquin River drainage basin where Hg TMDLs exist for the Sacramento-San Joaquin River Delta (Delta) and San Francisco Bay (Bay). Fish tissue targets for the MeHg in the Delta (0.24 mg kg^{-1} wet weight) and HgT in the Bay (0.20 mg kg^{-1} wet

weight) are for the protection of human health based on local consumption patterns [65,66]. Avian piscivores are also at risk of MeHg exposure from fish, with coastal and salt marsh birds in the western United States and Canada showing greater exposure than birds in terrestrial habitats [67]. The Bay and Delta TMDLs set numeric targets of 0.03 mg kg^{-1} (for MeHg in the Delta, HgT in the Bay) in small prey fish in an effort to protect foraging wildlife.

Although Bay and Delta TMDL targets do not apply directly to New Idria's immediate downstream watersheds, these examples provide state-wide context. For regional context, the Mendota Pool, which maintains an intermittent hydrologic connection to New Idria, is scheduled to adopt a TMDL in 2027 [61]. The work presented here will help address data gaps regarding Hg transport and loadings in this watershed.

2.4. Previous work

Prior research at New Idria has advanced our understanding of solid-phase Hg speciation in mining waste as it affects Hg mobility [23,24,28,35]. An early water quality study at New Idria demonstrated that the calcine waste piles are the primary source of Hg to San Carlos Creek, rather than AMD [13; Fig 5]. Additionally, Lowry et al. (2004) found that colloidal Hg particles may account for as much as 95% of the Hg released from calcine waste piles, enhancing downstream transport. Cross sectional sampling of floodplain and alluvial fan sediments [27] revealed large, stored inventories of Hg-rich sediment from historic mining debris. Sediment investigations conducted by EPA in 2010 also document the presence of mercury-contaminated sediments in floodplain deposits downstream from the mine [57]. Thus, remedial actions to improve mining-impacted waters and sediments downstream of New Idria must address multiple pollutant sources (e.g., AMD, calcines, channel sediments, floodplain deposits). A 1997–99 study established a baseline for Hg transport downstream from the New Idria Mine prior to on-site remediation actions in 2012 and 2015 [62,68]. Here we document water quality in San Carlos Creek after those interventions, as well as waters in Griswold and Panoche Creeks upstream from the New Idria flow path (Fig 3). We also begin to address information gaps identified in EPA's *New Idria Data Gaps Analysis Report* [57].

3. Methods

3.1. Sampling and analysis

We used established methods and the analytical tools listed in Table 1 to collect and analyze filtered (<0.22 μm) and unfiltered water samples from San Carlos Creek, Griswold Creek, and Panoche Creek (Fig 3). Sampling events took place in January, August, and October 2019 and in March 2020 to capture both wet and dry season conditions. Basic water quality parameters, including temperature, conductivity, pH, dissolved oxygen (DO), oxidation reduction potential (ORP), and turbidity, along with stream discharge, were measured in situ. The concentrations of HgT, MeHg, anions (Br^-, Cl^-, F^-, NO_2^-, NO_3^-, SO_4^{2-}) and suspended particulate matter (SPM), were determined using standard wet chemistry techniques and/or instrumentation, with references noted in Table 1. Both HgT and MeHg sample concentrations are reported as ng of Hg per liter of water (ng L^{-1}). Mercury analyses were calibrated using standards (75–125% recovery criterion) and data quality was assessed via ongoing precision and spike recovery analysis (85–115% recovery criterion), replicate sample analysis, and Milli-Q water blanks. Sample results were corrected for instrument blanks and the method detection limit (MDL), calculated as three times the standard deviation of blanks analyzed within the sample run, was 0.34 ± 1.1 pg Hg for HgT and 0.21 ± 0.08 pg Hg for MeHg A comprehensive description of our field sampling, sample processing, and analytical techniques is included in the Supporting Information.

3.2. Calculations for data interpretation

3.2.1. Particulate mercury estimates. Because we had limited filtered HgT (F-HgT) measurements, we use a simple linear regression of U-HgT versus SPM in AMD-impacted waters to estimate particulate Hg concentrations ($[Hg]_P$) from the regression slope (Fig 6). The standard error of the slope estimate yields the uncertainty in the $[Hg]_P$ estimate. This

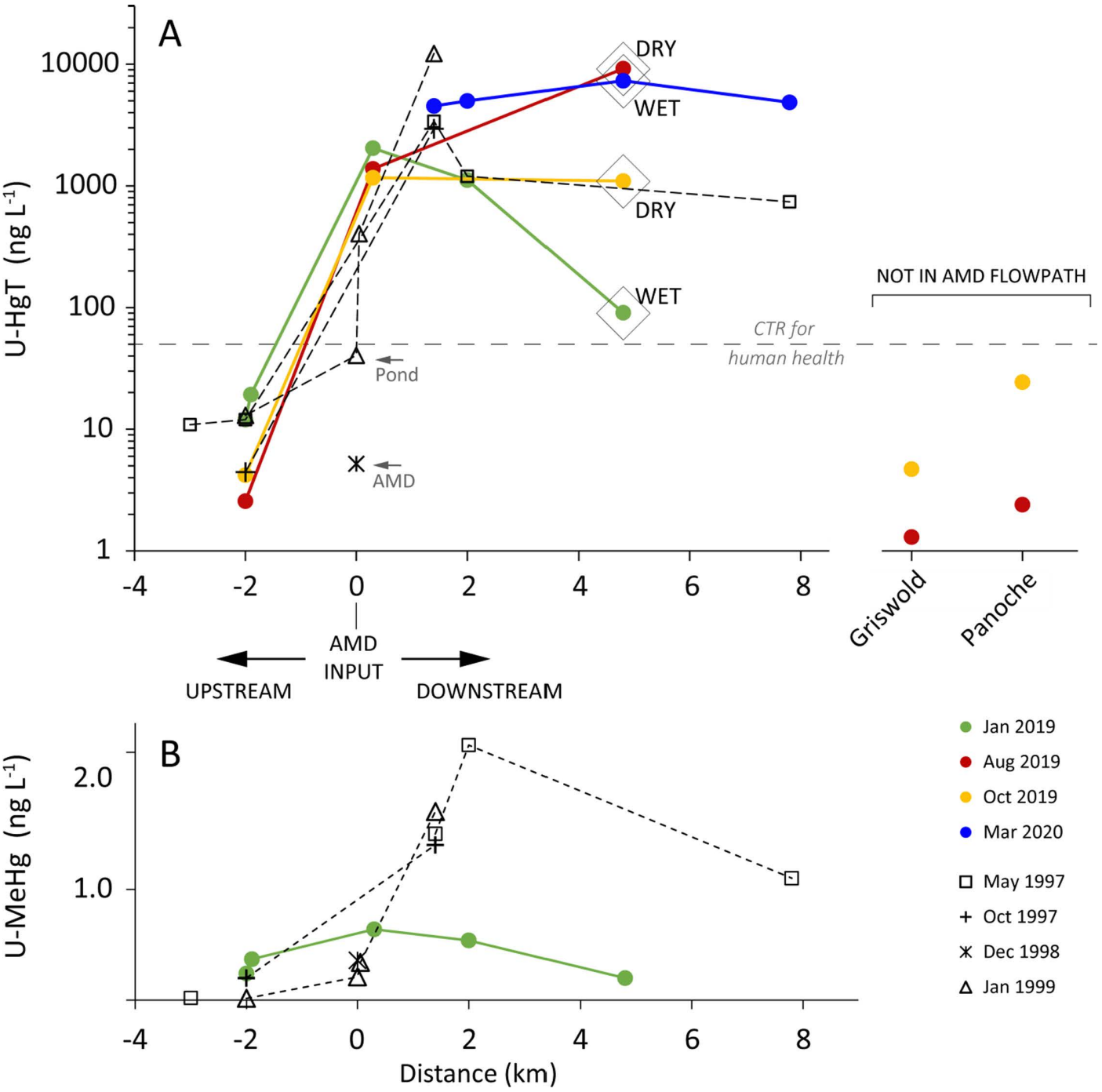

Fig 5. Unfiltered HgT and U-MeHg vs distance in San Carlos Creek (negative values are upstream of the mine) as well as U-HgT in Griswold and Panoche Creeks. Colored symbols are from this study; black and white symbols show 1997-99 data. The California Toxics Rule (CTR) water quality criteria for human health (50 ng L^{-1}) is shown as a dashed line on the U-HgT graph. Samples enclosed by diamonds reflect the atypical seasonal trends in Hg transport downstream from New Idria.

https://doi.org/10.1371/journal.pwat.0000328.g005

Table 1. Summary of methods.

Measurement/Activity	Technique	Application in this study	Reference
Trace metal clean sampling	Trace metal clean techniques	Avoid false positives via contamination	(Flegal et al., 1991; US EPA, 1996)
Sample filtration	EMD Millipore Sterivex-GP 0.22 μm polyethersulfone membrane filter, HDPE syringe	Quantify operationally defined dissolved concentrations	(Flegal et al., 1991)
Pore water sampling	MHE PushPoint sampler, c-flex tubing, HDPE syringe	Assess pore water geochemistry	(Zimmerman et al., 2005)
Total Mercury (HgT)	Cold vapor atomic fluorescence spectrometry (CVAFS), MERX-T	Quantify Hg concentrations	EPA Method 1631 (US EPA, 2002)
Monomethylmercury (MeHg)	Distillation & CVAFS, MERX-M	Quantify MeHg concentrations, assess Hg methylation potential	EPA Method 1630 (USEPA, 2001)
Anions	Ion chromatography	Provide watershed context	EPA Method 300.1 (US EPA, 1997)
Suspended particulate matter (SPM)	Benchtop filtration	Demonstrate particulate Hg transport, calculate K_d	ASTM D5907 – 18 (ASTM, 2018)
*Basic water quality parameters	YSI ProDSS multi-parameter water quality field probe	Provide context for other geochemical parameters	(Gibs et al., 2007)
Stream discharge	Salt slug, conductivity sensor	Quantify chemical transport	(Kite, 1993, 1989)

*Temperature, conductivity, pH, dissolved oxygen (DO), oxidation reduction potential (ORP), turbidity.

https://doi.org/10.1371/journal.pwat.0000328.t001

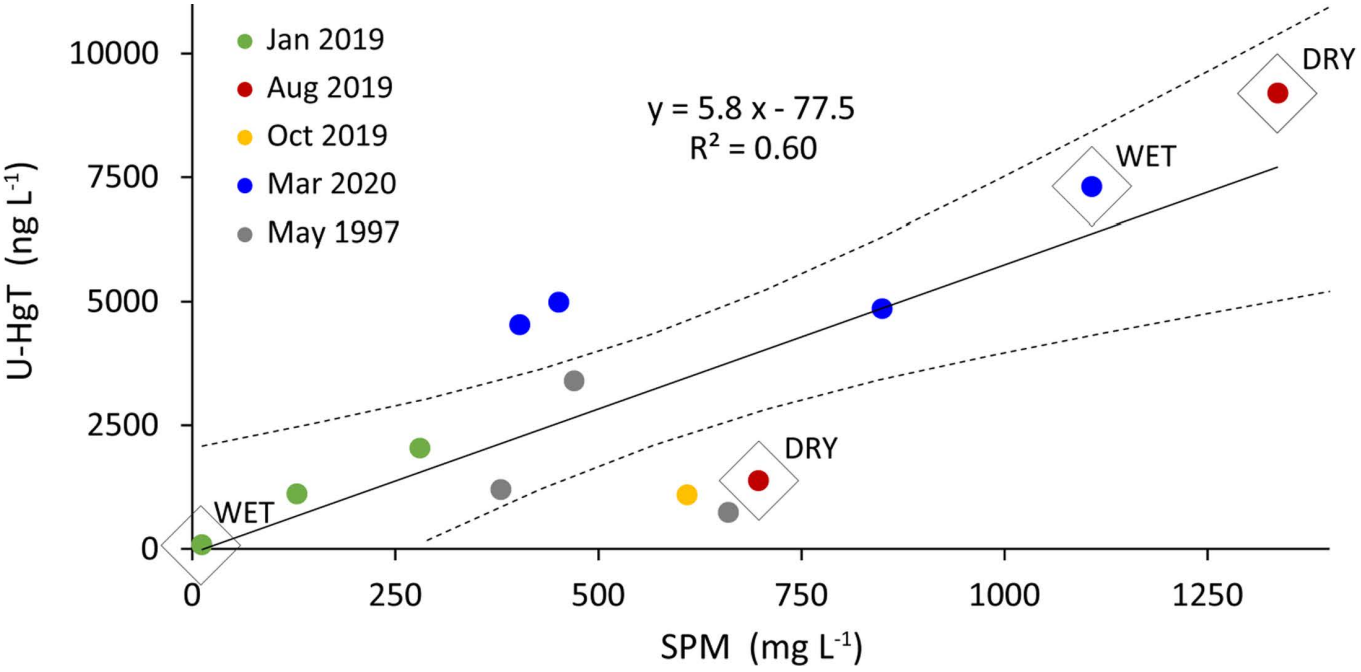

Fig 6. Linear regression (solid line) showing the 95% confidence interval (dashed lines) for U-HgT vs suspended particulate matter (SPM) in San Carlos Creek downstream from New Idria (upstream samples are not included). Colored symbols are from this study; grey symbols show 1997 data. Diamonds enclose samples collected ~5 km downstream from the mine and demonstrate the inconsistent seasonal U-HgT trends.

https://doi.org/10.1371/journal.pwat.0000328.g006

approach assumes the proportion of F-HgTis small relative to U-HgT, which holds true for samples with elevated SPM concentrations (>100 mg L^{-1}).

3.2.2. Particulate-dissolved distribution coefficient (K_d). The particulate-dissolved distribution coefficient (K_d) is the ratio of particulate phase to dissolved phase concentrations of an atom or molecule at equilibrium. We calculated the K_d for HgT using the following equation:

$$K_d = \frac{[Hg]_p}{[Hg]_d} \tag{1}$$

where $[Hg]_p$ is the particulate phase Hg concentration (mg kg^{-1}) and $[Hg]_d$ is the concentration of Hg in the dissolved phase (mg L^{-1}), operationally defined as the concentration in filtered (<0.22 μm) water samples. The units for K_d are L kg^{-1} and values are commonly reported as log K_d.

In Equation 1, $[Hg]_p$ is calculated by accounting for filtered concentrations using the following equation:

$$[Hg]_p = \frac{([UHg] - [FHg])\ (mg\ L^{-1})}{[SPM]\ (kg\ L^{-1})} \tag{2}$$

Typical log K_d values for HgT range from 5 to 7, i.e., from 10^5 to 10^7 particulate Hg atoms for every dissolved atom [69]. Lower log K_d values for HgT may indicate solubilization, or a system that is not at equilibrium. Note that our K_d calculations require filtered concentrations, which are not available for all sampling events. We therefore report fewer K_d values in Table 2 than estimates of particulate Hg concentrations ($[Hg]_p$) in Fig 6.

3.2.3. Stream discharge. In March 2020 surface water discharge was quantified 2 km downstream from the mine using the salt slug injection method [70,71]. A known volume of salt dissolved in creek water was added to the creek as a near-instantaneous slug, while electrical conductivity (EC) was recorded downstream using a water meter. The area under the conductivity versus time breakthrough curve was then used to calculate stream discharge via the equation:

$$Q = \frac{M_s}{\int_0^T (C_t - C_0)\, dts} \tag{3}$$

where Q (m^3 s^{-1}) is stream discharge, M_s (kg) is the mass of salt added to the stream, T(s) is the time it takes for the salt slug to move through the stream, C_t (kg m^{-3}) is the salt concentration in the stream at time t as the salt slug moves, and C_0 is the background concentration of salt in the water before the salt slug is added, estimated by stream salinity.

Table 2. Total mercury (HgT), monomethylmercury (MeHg), suspended particulate matter (SPM), and log K_d.

Location	Distance (km)	UHgT (ng L^{-1})	FHgT (ng L^{-1})	% Filtered	UMeHg (ng Hg L^{-1})	% MeHg	SPM (mg L^{-1})	Log K_d
Upstream	-2	2.6 - 19.3	1.3 - 3.0	31 - 80	0.24 - 0.37	2	2 - 3	5.2
Mixing Zone	0.3	1,170 - 2,050	78 - 154	9 - 13	0.64	0.03	280 - 700	4.2
Downstream	1 - 8	91 - 9,200	5 - 22	0.1 - 2	0.20 - 0.54	0.2	12 - 1,300	4.9 - 6.0
Griswold Creek	NA	1.3 - 4.7	1.4 - 2.7	57 - 100	--	^	85	^
Panoche Creek	NA	2.4 - 24	1.1	5	--	^	2 - 3	6.9

single values indicate n = 1 (see Supporting Table 1 for full data set).

negative distance values represent sites upstream from the mine.

-- sample not analyzed or not collected.

^ data not available for calculation.

NA: not applicable (stream is not in New Idria flow path).

https://doi.org/10.1371/journal.pwat.0000328.t002

4. Results

The data we describe can be broadly broken into four zones: (1) upstream San Carlos Creek (i.e., water upstream of New Idria); (2) the AMD mixing zone where pH and ORP change rapidly; (3) downstream San Carlos Creek, between the mixing zone and the Silver Creek Wetland; and (4) the portion of the lower Panoche Creek watershed that is outside the New Idria flow path (i.e., Griswold and Panoche Creeks; Fig 3). Below and in Table 2, we summarize concentration ranges for analytes in these zones, with detailed concentrations reported in S1 and S2 Tables.

4.1. Total mercury (HgT), monomethylmercury (MeHg), and suspended particulate matter (SPM)

U-HgT concentrations ranged from approximately 1–25 ng L^{-1} in streams not impacted by discharge from the New Idria Mine, including San Carlos Creek upstream of New Idria and sites along Panoche and Griswold Creeks (Table 2; Fig 5). SPM at these sites was consistently <15 mg L^{-1}, with the exception of Griswold Creek in August 2019, which was 85 mg L^{-1} (Table 2).

U-HgT in downstream San Carlos Creek spanned two orders of magnitude, with values as low as 91 ng L^{-1} and as high as 9,200 ng L^{-1}. Although U-HgT in mine-impacted stream water was notably elevated when we sampled while it was raining in March 2020 (~4,500–7,300 ng L^{-1}), we observed the lowest U-HgT concentrations along this reach in January 2019 (~100–1,000 ng L^{-1}), immediately after the largest storm event that occurred during this study.

Similar to U-HgT, SPM concentrations were highly variable downstream from the mine, with the lowest SPM value comparable to upstream water (<15 mg L^{-1}) and the highest exceeding 1,300 mg L^{-1} (Table 2). SPM and U-HgT were positively correlated along this reach of San Carlos Creek ($R^2 = 0.60$; Fig 6) and most of the Hg was associated with particles ($K_d \sim 10^5$). For sampling events when both filtered and unfiltered water was collected, F-HgT accounted for ~10% of the HgT concentration in the AMD mixing zone immediately downstream from the mine. This could be due to reduced pH in the mixing zone or could indicate colloidal Hg [24]. At sampling sites located more than a kilometer downstream, F-HgT comprised ≤2% of HgT. In contrast, F-HgT accounted for 60–100% of the HgT in the groundwater-fed pool in the Griswold Creek channel.

Unfiltered MeHg (U-MeHg) in San Carlos Creek was sampled in January 2019, and concentrations ranged from 0.20-0.37 ng L^{-1}. Average upstream concentrations (0.3 ng L^{-1}) were slightly lower compared to downstream (0.5 ng L^{-1}). In general, the percentage of U-MeHg relative to U-HgT was low (≤2%).

4.2. pH and oxidation reduction potential

The similarity of pH trends observed in the late 1990s and in 2019–20 suggest ratio of AMD to total stream flow in San Carlos Creek has remained relatively stable at about 40–45% (S2 Table and Fig 7A). Upstream of New Idria, pH was elevated (8.5–8.9). We did not have access to the settling pond but assume the pH of AMD entering the creek is ~3 [13]. The introduction of the AMD depressed the pH of San Carlos Creek to values ranging from 6.2 to 7.1. The pH increased to ~8 about a kilometer further downstream. Oxidation reduction potential (ORP) data indicated oxidizing conditions upstream of the mine (140–300 mV), reducing conditions in the mixing zone (-5 to -110 mV), and a return to oxidizing conditions (160–290 mV) beyond the mixing zone (Fig 7B). Based on historic observations of a strong hydrogen sulfide (H_2S) odor at the mine opening combined with low ORP in the mixing zone, we infer conditions are strongly reducing in the acidic, sulfidic AMD waters. Griswold Creek had lower pH and ORP values (~7.3 and 100 mV, respectively) compared to Panoche Creek (~7.8 and 250 mV, respectively).

4.3. Major anions and stream discharge

Dry season mean concentrations of sulfate (mg SO_4^{2-} L^{-1}), chloride (mg Cl^- L^{-1}, fluoride (mg F^- L^{-1}), and bromide (mg Br^- L^{-1}) in the headwaters of San Carlos Creek upstream from the mine were 51, 16, 0.05, and 0.2 mg L^{-1},

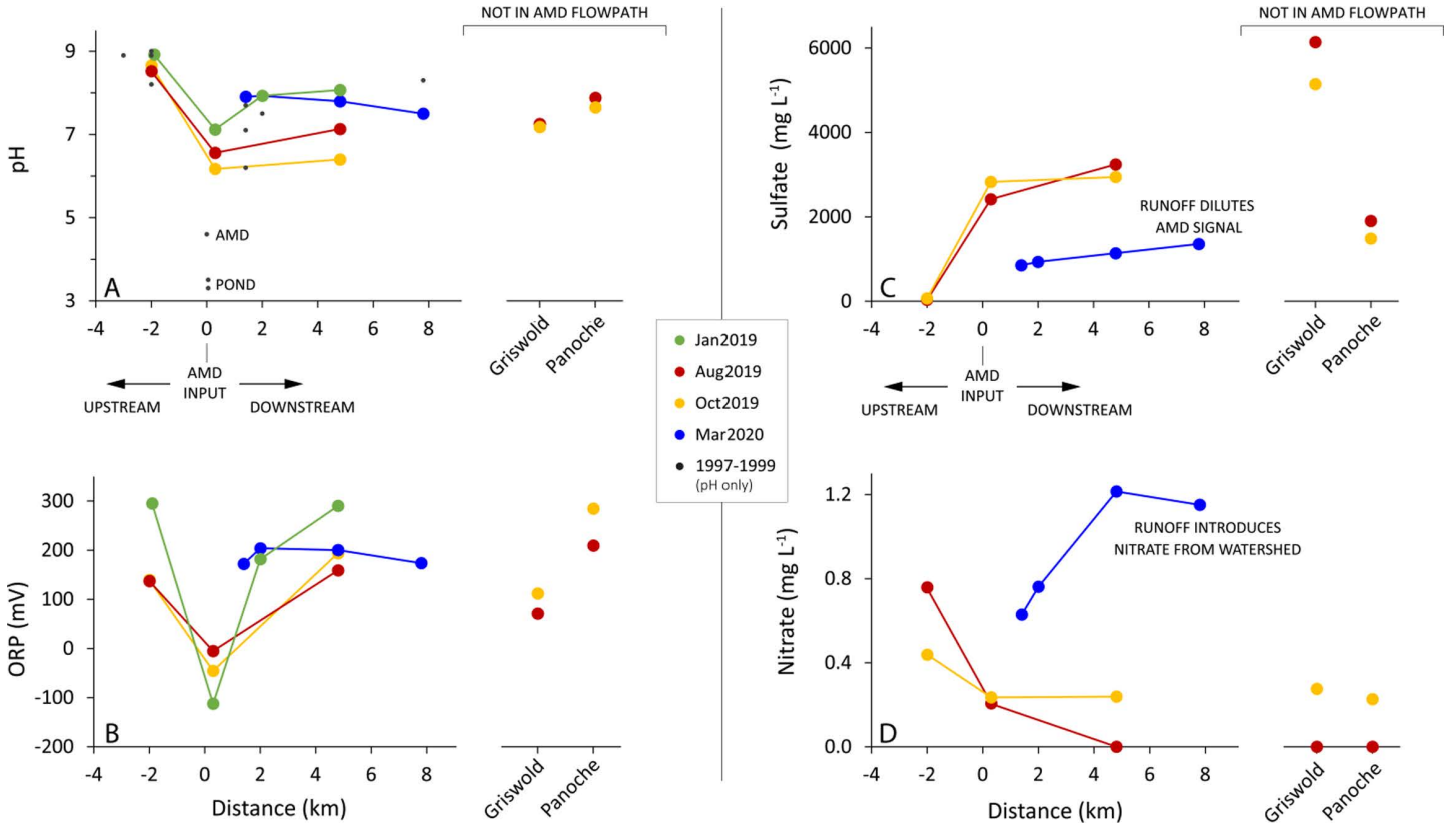

Fig 7. Select ancillary parameters (pH, ORP, sulfate, and nitrate) versus distance in San Carlos Creek. Black dots on the pH graph indicate historic data (1997-99) and negative distance values indicate sampling locations upstream from New Idria.

https://doi.org/10.1371/journal.pwat.0000328.g007

respectively (Tables 3 and S2 Table). These values increased by 1–2 orders of magnitude after AMD entered the stream, with sulfate increasing by more than 50-fold, reaching concentrations as high as 3,200 mg L^{-1}. Although Panoche Creek was sampled outside the AMD-flow path, anion concentrations in this stream were comparable to AMD-impacted creek water, with values 5–33 times higher than upstream of the mine. In Griswold Creek, this suite of anions occurred at concentrations ~2–5 times higher than in Panoche Creek, with sulfate and chloride as high as 6,140 mg L^{-1} and 495 mg L^{-1}, respectively. Dry season nitrate (NO_3^-) and nitrite (NO_2^-) concentrations were typically undetectable.

During the March 2020 rain event, only downstream San Carlos Creek stations were sampled. Stream discharge 2 km from New Idria was 32 L s^{-1} and the Panoche 2W weather station (USC00046675, Fig 3) recorded 1.7 cm of precipitation on that day. Anions other than nitrate and nitrite were diluted, with concentrations about 2–3 times lower relative to dry season conditions. Nitrate concentrations were 0.6 mg L^{-1} near the mine and steadily increased to 1.2 mg L^{-1} at a distance of 7.8 km, while nitrite remained below the detection limit (<0.2 mg L^{-1}). Griswold and Panoche Creeks were not sampled during the wet season.

5. Discussion

Recent data compared to measurements made over 25 years ago confirm ongoing AMD (Section 5.1) and Hg (Section 5.2) discharges to San Carlos Creek.

Table 3. Basic water quality parameters and anion concentrations.

Location	Distance (km)	pH	ORP (mV)	Conductivity (mS cm^{-1})	Temp (°C)	Turbidity (FNU)	NO_3^- (mg NO_3^- L^{-1})	SO_4^{2-} (mg SO_4^{2-} L^{-1})	F^- (mg F^- L^{-1})	Cl^- (mg Cl^- L^{-1})	NO_2^- (mg NO_2^- L^{-1})	Br^- (mg Br^- L^{-1})
Upstream	-2	8.5 - 8.9	140 - 300	0.7 - 0.9	9 - 15	<1 - 15	0.4 - 0.8	35 - 66	0.05 - 0.07	14 - 17	0.40	<0.23
Mixing Zone	0.3	6.2 - 7.1	-110 - -5	1.8 - 3.2	12 - 21	70 - 260	<0.3	2,150 - 2,830	0.1 - 4	56 - 90	<0.2	0.36 - 0.50
Down-stream	1-8	6.4 - 8.1	160 - 290	1.3 - 4.5	8 - 19	3 - 2,350	0.6 - 1.2	850 - 3,240	0.7 - 1	34 - 83	<0.2 - 0.2	0.28 - 0.45
Griswold Creek	NA	7.2 - 7.3	70 - 110	8.6 - 9.2	14 - 20	55 – 65	<0.3 - 0.3	5,140 - 6,140	2.7 - 3.4	446 - 495	<0.2 - 0.3	2.6 - 2.8
Panoche Creek	NA	7.7 - 7.9	210 - 290	2.7 - 3.9	8 - 20	<1	<0.3	1,490 - 1,900	0.6 - 0.7	230 - 309	<0.2	1.0 - 1.2

single values indicate n = 1 (see Supporting Table 2 for full data set).

negative distance values represent sites upstream from the mine.

NA: not applicable (stream is not in New Idria flow path).

https://doi.org/10.1371/journal.pwat.0000328.t003

5.1. Acid mine drainage and the San Carlos Creek mixing zone

AMD adds to San Carlos Creek flow, depresses pH and ORP, increases the concentration of sulfate, and forms an Fe or Fe/Al flocculant (Fe-flocs) when it mixes with creek water [57,58,72]. Each of these impacts degrade downstream water quality.

Iron and salts introduced by AMD result from the oxidation of Fe-bearing S^{2-} minerals, such as pyrite [73]. Sulfate, from the oxidation of S^{2-}, as well as other salts, such as Cl^- and F^-, increase in San Carlos Creek as a result of mixing with AMD. Amorphous iron-oxyhydroxysulfates or, depending on pH conditions, white aluminum-hydroxysulfates form in the mixing zone [58]; S4 Fig. This material covers the channel bottom, impairing ecological function by physical smothering [74]. The Fe-flocs also provide binding sites for metals, such as Hg, and play an important role in metals transport and fate.

Previous investigations reported U-HgT concentrations of <200 ng L^{-1} and a pH between 3.3 and 4.6 in AMD at the adit and in pond water [13,25,57]; S1 Table. While AMD drastically alters water chemistry in San Carlos creek, it is not a significant source of Hg. Although we did not have access to the pond in 2019–20, the similarity between historic and recent pH trends suggests the ratio of creek water to AMD has remained consistent over time, with AMD comprising about 40–45% of the downstream flow [13]. The relatively low HgT log K_d (~4) in the mixing zone relative to water further downstream (log K_d of 5–6; Table 2) likely reflects disequilibrium in the mixing zone. Mercury solubilized under acidic (ph < 4) conditions upstream of the mixing zone may not have sufficient time for complete adsorption within the mixing zone.

5.2. Persistent mercury transport from New Idria

Historic (1997–99) and recent (2019–20) sampling events confirm the persistent transport of Hg from the New Idria Mine to downstream wetland habitats. These recent and historic measurements capture California's seasonal variability, providing insights about within-channel and watershed processes. Intriguingly, U-HgT concentrations downstream from New Idria are not always higher in the wet season relative to dry season conditions, as shown by our Jan 2019 results compared to Aug and Oct 2019 (Fig 5). This seasonal trend is the opposite of monitoring results downstream from the former New Almaden Mercury Mine in San Jose, CA, and the former Gambonini Mercury Mine near Petaluma, CA, where wet weather discharges are typically associated with peak U-HgT concentrations (Mckee et al., 2018; Whyte and Kirchner, 2000). Evaluating correlations between U-HgT and SPM can help explain why seasonal patterns of Hg transport downstream from New Idria are different compared to other coast range Hg mines where AMD is not generated, such as the New Almaden and the Gambonini Mines.

5.2.1. Within-channel processes explain seasonal mercury and SPM trends. Downstream from New Idria, Hg and SPM concentrations in San Carlos Creek are controlled by the interplay between Fe-flocs from AMD, Hg leached from calcines, and seasonal changes in streamflow. A linear regression analysis indicates that 60% of the variance in U-HgT downstream from the mine is driven by changes in SPM, with estimated particulate Hg concentrations in the range of 3.6 – 7.8 μg g^{-1}, based on the 95% confidence interval of the slope in Fig 6. The outliers to the best fit regression of U-HgT vs SPM demonstrate there is variability in the composition of SPM. All three of the outliers below the 95% confidence interval of the regression (yellow, grey and red points) were collected during the dry season, when SPM was observed to be predominantly amorphous Fe-flocs that could remain suspended at low flows. The two outliers above the regression 95% confidence interval (blue points) were collected in the wet season, when coarser sediments, including weathered calcines, can be suspended by higher flow velocities.

The finding that U-HgT correlates to SPM is common in mining impacted watersheds [14,18]. However, the two distinct modes of transport for Hg from New Idria – AMD Fe-flocs vs weathered calcines – create distinct seasonal patterns in San Carlos Creek. Lighter Fe-floc particles easily remain suspended during low flows, leading to the atypical observation downstream from New Idria: elevated SPM and U-HgT in dry season samples, as well as in higher flow samples (Fig 5).

The inconsistency in dry and wet weather can clearly be seen in the range of concentrations observed ~5km downstream from New Idria, where we sampled multiple times (Figs 5, 6 and and S4 Fig). Considering how easily the flocculant can be resuspended, the notably low U-HgT and SPM concentrations recorded at that distance in January 2019 make sense (90 ng L^{-1} and 11.5 mg L^{-1}, respectively). Over 4 cm of precipitation was recorded at the Panoche 2W weather station the week preceding our January 2019 sampling event. Additionally, discharge at the USGS Panoche Creek gaging station reached 2.5 m^3 s^{-1} on January 18, 2019, the maximum value recorded over the course of this study – we began sampling on January 20, 2019 (S1 Table). Elevated stream flow likely scoured the channel bottom, resuspending flocculant as a source of particulate Hg, and we sampled before a new flocculant layer had time to form. Hg concentrations may have been further diluted by overland flow and particulate inputs from tributaries.

U-HgT concentrations were consistently high (4500–7300 ng L^{-1}) in March 2020, when we sampled while it was raining. However, the highest U-HgT (9200 ng L^{-1}) and SPM (1340 mg L^{-1}) were recorded in August 2019, during the dry season (Fig 5 and S1 Table). Although that data point exists as an outlier for the observed dry season trends, it is explained by the corresponding SPM results. The elevated paired U-HgT and SPM data suggest that the sampling captured real stream conditions at that time and location. Common events such as wind, cattle, wildlife, vehicles can create episodic turbulence that resuspends the bed flocculent.

5.2.2. Anion data further reflect the impacts of mining and land use. Major anion concentrations and ratios (Table 3) reflect watershed processes. During wet weather, surface flows introduced nitrate from the surrounding pasturelands, and concentrations in San Carlos Creek increased from 0.6 to 1.2 mg L^{-1} along the ~ 8 km reach we sampled. In contrast, sulfate concentrations were highest in the dry season and reflect the influence of AMD on water chemistry. Upstream sulfate concentrations were about 50 mg L^{-1} and increased drastically to >2000 mg L^{-1} in the mixing zone (Table 2S). Downstream concentrations remained elevated but were slightly diluted by surface runoff in March 2020. The high concentrations of oxidized sulfur and Hg entering downstream wetlands may enhance Hg methylation by sulfate reducing bacteria [75,76]. Excessive sulfate stimulation (i.e., above 20 mg L^{-1}) can also inhibit Hg methylation if the resulting sulfide concentrations are high enough to reduce Hg bioavailability [77,78]. As discussed below, sulfate stimulation appears to promote mercury methylation that is countered by demethylation.

5.2.3. Transported mercury is readily methylated. MeHg concentrations in water indicate that Hg transported by San Carlos Creek is available for methylation. Anaerobic microbial methylation in San Carlos Creek may occur in streambed sediments as well as in microzones within Fe-flocs or other particles suspended in the water column [79–81]. Methylation in the hyporheic zone, where groundwater and surface water interact below the streambed, can also introduce MeHg to surface waters [82]. The abundance of sulfate, along with the potential for low oxygen concentrations within

the fine grained Hg-rich flocculant on the streambed, likely promotes methylation via sulfate reducing bacteria [83]. The depletion of sulfate in pore water (2,150 mg L^{-1}) compared to overlying water (2,830 mg L^{-1}) in Oct 2019 (S2 Table) may be an indication of sulfate reduction in channel sediments. The abundance of oxidized Fe(III) may also support MeHg production by iron-reducing bacteria [84].

The fraction of U-HgT present as U-MeHg (%MeHg) is considered an indicator of net ecosystem methylation efficiency, and represents the balance of Hg methylation relative to the demethylation of MeHg [77,85]. Low (<5%) fractions of MeHg are typically indicative of low net methylation efficiency in a waterbody. However, in mining-impacted waters, the grossly elevated denominator ([HgT]) relative to most natural systems drives this value [85] and low (<1%) fractions of MeHg relative to HgT in downstream San Carlos Creek are not necessarily associated with low methylation rates.

In San Carlos Creek, high MeHg demethylation rates may counter high methylation efficiency. Sediments in this stream have some of the highest MeHg demethylation rates measured in a comparison across a gradient of contaminated ecosystems [49]. Increased microbial demethylation rates facilitate growth by reducing soluble Hg(II) to GEM [86]. Thus, even though the raw ingredients for MeHg production are abundant – sulfate, inorganic Hg, and low ORP – the feedback loop of microbial demethylation attenuates MeHg accumulation to <1% of the total.

5.2.4. Potential biological impacts. Biological data shedding light on ecosystem effects of MeHg downstream of New Idria are not available, to our knowledge. However, isotope data confirm that Hg from the mine is taken up by local vegetation [28]. Food web complexity in San Carlos Creek is severely limited because Fe-flocs cover stream sediments, reducing the benthic invertebrate population to a limited number of oligochaets (i.e., earthworms) that can tolerate low oxygen and pollutants [57]. However, contaminants from New Idria travel through other tributaries and can potentially reach riparian wetlands. Dryland streams, such as those in the Panoche Creek watershed, provide habitat for many species of plants and animals [87] and the wetlands downstream from New Idria provide unique habitat in this desert ecosystem (Fig 2). The ongoing release of Hg from New Idria, transport downstream through San Carlos Creek, and filtration through wetland vegetation and sediment, introduces the potential for transfer to higher trophic levels of associated desert food webs. During the rare years when surface water hydrologic connectivity exists all the way to the Mendota Pool area, the ecosystem of the San Joaquin River containing higher trophic level fish could potentially be affected.

The endangered California Condor (*Gymnogyps californianus*) has been re-introduced at Pinnacles National Monument, 45 km to the west and within soaring and foraging range of New Idria [88]. Demonstrated Hg exposure to condors in the Pacific Northwest raises questions about risks to re-introduced California Condors near New Idria [89]. Although California Condors prefer large carrion, smaller animal carcasses such as rabbits, coyotes and foxes also provide food and can form connections from Hg-contaminated wetlands to the local food web. Arctic tundra islands foxes showed Hg concentrations in fur as high as 20–30 mg kg^{-1} as a result of feeding on birds from marine organisms with 1–4 mg kg^{-1} Hg in their tissue [90]. A great deal of Hg-based research and regulatory effort in California has focused on San Francisco Bay, the Bay Delta, and on lake reservoir and stream ecosystems that people and wildlife rely on for fish. The potential food web impacts of Hg-contamination in perennial wetlands that serve a desert ecosystem within the Coast Ranges has not been extensively explored.

5.3. Complex downstream transport processes

Downstream transport of HgT beyond Silver Creek through the Panoche Creek alluvial fan is not well characterized, nor are floodplain HgT inventories. A 2010 EPA investigation showed that sediments in the Silver Creek floodplain to its confluence with Panoche Creek had HgT concentrations of 0.1 – 12 mg kg^{-1} [57], compared to our estimate of ~6 mg kg^{-1} HgT for particles transported in San Carlos Creek (Fig 6). Those higher concentration sediment deposits represent a larger inventory that, according to Rytuba (2015), may be mobilized to downstream ecosystems during extreme winter storm conditions.

In the conceptual model for New Idria's impacts to downstream ecosystems THg loads vary over the relatively short timescales of dry and wet years, as well as longer timescales of extreme weather events that are likely to increase in frequency and severity with climate change [91]. Although Panoche Creek ends within the Panoche Fan most years (Fig 3), the USGS gauge at Panoche Creek (11255575) shows that flow events most likely to convey sediments all the way to the Mendota Pool via the Fresno Slough have occurred six times in the past 25 years (e.g., > 15 m^3 s^{-1} or ~500 cfs; S1 Fig). During such high flow periods the Mendota area often experiences flooding, with flow direction further confounded by agricultural withdrawals from the Mendota Pool. As a result, sediment transport and depositional processes in Mendota are complex. Sharma and Weinman [92] found that sediments in the Mendota Pool are enriched in Hg relative to background (0.94 to 6.91 mg kg^{-1}), but the downstream fate of HgT loads to the San Joaquin River watershed from New Idria remain a mystery. Ecosystem receptors are not well defined and biota Hg concentrations are not readily available, with the exception of the 2005 fish tissue survey [93].

6. Conclusions

The history of mining at New Idria resulted in two contaminant sources that continue to impact the local watershed: acid mine drainage (AMD) and solid waste piles of calcines. Although low pH AMD is now routed underground to reduce its contact with on-site waste, it continues to discharge to the creek year-round, with San Carlos Creek and the Silver Creek Wetland, located about 10 km from New Idria, functioning as a de-facto AMD treatment system. While the AMD introduces metals and salts to the creek, the above-ground calcine piles are the primary source of Hg. Although this Hg is available for methylation, the percentage of HgT present as MeHg in San Carlos Creek is kept low (<1% of HgT) by the relatively high HgT concentration and elevated microbial demethylation rates.

Mercury from New Idria moves downstream with suspended particles that include a mix of Fe flocs, weathered calcines, and native sediments. The resulting mix has an average HgT concentration of 5.8 mg kg^{-1} and reaches the 0.25 km^2 (60-acre) Silver Creek Wetland, which is only ~10 km downstream. Topography and visual observation show that lower Silver Creek frequently flows another 25 km to the 0.65 km^2 (160-acre) Panoche Creek Wetland and, during high discharge events, the overflow channel of Panoche Creek reaches the Fresno Slough (Fig 3).

The intermittent hydrologic connection between New Idria and the Fresno Slough suggests that an assessment of Hg loads and impacts from this mine will be more involved and require more extensive investigation than the storm hydrograph sampling approach exemplified by Mckee et al. (2018) downstream of the New Almaden Mine. While HgT transport within San Carlos Creek is well documented, substantive data gaps remain regarding downstream impacts, including: (1) inventorying the > 100 years of Hg stored in floodplain deposits, (2) quantifying Hg transport in the Mendota area, and (3) assessing ecological impacts, including Hg bioaccumulation into aquatic and terrestrial biota, in downstream riparian wetlands and in the Fresno Slough, Mendota Wildlife Area, Mendota Pool, and the San Joaquin River. A combined geomorphic and geochemical assessment will be needed to quantify floodplain inventories while hydrologic and sediment transport modeling can create a framework of Hg mobilization risks associated with increasing droughts and storm intensities. Geochemical tools, such as isotopic tracers of Hg and element ratios [e.g., Sr depletion and Rb/Sr ratios; 94], may help with source identification.

EPA's settlement agreement [62] directs the PRP named at New Idria to develop a remedial investigation (RI) that includes a human health and ecological risk assessment. Those RI elements may address some of the gaps described above, although the full geographic scope and extent of the RI is not clearly defined. Research by the authors, the community of scientists cited in this paper, and new entrants to the field will continue to augment and support the regulatory process. California's mining-impacted watersheds present a twenty-first century challenge to rehabilitate natural resources impaired by historic resource extraction that founded the state's economy.

Key Points

- Mercury and acid mine drainage (AMD) from the former New Idria mine are transported to riparian wetland habitat.
- Seasonal patterns of contaminant transport downstream from New Idria are not typical of most cinnabar mines due to the nature of the AMD-derived flocculant.
- The New Idria flow path intermittently reaches the Fresno Slough near the Mendota Pool, but the extent of mercury transport remains unknown.

Supporting information

S1 Fig. (A) Annual precipitation from the National Oceanic and Atmospheric Administration (NOAA) online climate data for the Panoche 2W Station (USC00046675). Red dots indicate sampling events from this investigation. (B) Flow at USGS Gauge 1125555 along Panoche Creek.
(PDF)

S2 Fig. The Panoche Valley and Vallecitos Valley Groundwater Basins showing flow from New Idria toward Silver Creek and the groundwater basin [59].
(PDF)

S3 Fig. San Carlos Creek approximately 5 km downstream from New Idria in June 2017 (before the drought ended), January 2019, when we sampled after a large storm, and March 2020 when we sampled in moderate rainfall.
(PDF)

S4 Fig. (A) San Carlos Creek in April 2020 about 5 km downstream showing the typical orange colored water. (B) In Aug, 2019, water in the mixing zone was white, presumably from the precipitation of aluminum hydroxysulfates. (C) Water in San Carlos Creek upstream from New Idria. (D) View of San Carlos Creek flowing along the tow of a calcine waste pile.
(PDF)

S1 Table. Summary of Data: Mercury, SPM, K_d, and Flow Rate.
(PDF)

S2 Table. Summary of Data: Basic Water Quality and Anions.
(PDF)

Acknowledgments

The authors are grateful to members of the CSUN Water Science Program, especially Cindy De Jesus Bartolo, Kyle Ikeda, Greg Jesmok, Philippe Leguellec, and Hannah Sloan for their field and analytical support and thank Dr. Hilde Schwartz for help with site access. This work was supported with project funding from the CSU Water Resources and Policy Initiative (WRPI, now CSU WATER) and from CSUN's College of Math and Science and College of Social and Behavioral Sciences. Graduate student support was provided by the Geological Society of America (GSA) and from CSUN's Office of Graduate Studies, Association of Retired Faculty, and Department of Geological Sciences Hanna Fellowship Program. We also thank the anonymous reviewers for their time and feedback. This manuscript is dedicated to the memory of Francis Katherine (Kate) Woods (1957–2017) and Kemp Minor Woods (1953–2018), benitoite miners who provided

safe harbor in the badlands for a multitude of students, researchers, and off-road enthusiasts for three decades and were an essential source of site knowledge and history.

Author contributions

Conceptualization: Rachel Hohn, Khalil P Abusaba, Erin N Bray, Scott C Hauswirth, Carl H Lamborg, Priya M Ganguli.

Data curation: Rachel Hohn, Erin N Bray, Robert P Mason, A Russell Flegal, Priya M Ganguli.

Formal analysis: Rachel Hohn, Khalil P Abusaba, Scott C Hauswirth, Byran C Fuhrmann, Priya M Ganguli.

Funding acquisition: Rachel Hohn, Erin N Bray, Scott C Hauswirth, Priya M Ganguli.

Investigation: Rachel Hohn, A Russell Flegal, Priya M Ganguli.

Methodology: Rachel Hohn, Khalil P Abusaba, Byran C Fuhrmann, Marc W Beutel, Carl H Lamborg, Priya M Ganguli.

Project administration: Rachel Hohn, Priya M Ganguli.

Resources: Rachel Hohn, Marc W Beutel, Robert P Mason, A Russell Flegal, Priya M Ganguli.

Supervision: Rachel Hohn, Marc W Beutel, Priya M Ganguli.

Validation: Rachel Hohn, Khalil P Abusaba, Robert P Mason, Priya M Ganguli.

Visualization: Rachel Hohn, Khalil P Abusaba, Erin N Bray, Carl H Lamborg, Priya M Ganguli.

Writing – original draft: Rachel Hohn, Scott C Hauswirth.

Writing – review & editing: Rachel Hohn, Khalil P Abusaba, Erin N Bray, Scott C Hauswirth, Byran C Fuhrmann, Marc W Beutel, Carl H Lamborg, Robert P Mason, A Russell Flegal, Priya M Ganguli.

References

1. Streets DG, Horowitz HM, Lu Z, Levin L, Thackray CP, Sunderland EM. Five hundred years of anthropogenic mercury: spatial and temporal release profiles*. Environ Res Lett. 2019;14(8):084004. https://doi.org/10.1088/1748-9326/ab281f
2. Keane S, Bernaudat L, Davis KJ, Stylo M, Mutemeri N, Singo P, et al. Mercury and artisanal and small-scale gold mining: Review of global use estimates and considerations for promoting mercury-free alternatives. Ambio. 2023;52(5):833–52. https://doi.org/10.1007/s13280-023-01843-2 PMID: 36897513
3. Dai MQ, Geyman BM, Hu XC, Thackray CP, Sunderland EM. Sociodemographic Disparities in Mercury Exposure from United States Coal-Fired Power Plants. Environ Sci Technol Lett. 2023;10(7):589–95. https://doi.org/10.1021/acs.estlett.3c00216 PMID: 37455865
4. Krabbenhoft DP, Sunderland EM. Environmental science. Global change and mercury. Science. 2013;341(6153):1457–8. https://doi.org/10.1126/science.1242838 PMID: 24072910
5. Gębka K, Bełdowski J, Bełdowska M. The impact of military activities on the concentration of mercury in soils of military training grounds and marine sediments. Environ Sci Pollut Res Int. 2016;23(22):23103–13. https://doi.org/10.1007/s11356-016-7436-0 PMID: 27591883
6. Gilbert C. Prospectors, capitalists, and bandits: the history of the New Idria quicksilver mine, 1854-1972. San Jose, CA: San Jose State University; 1984.
7. Fitzgerald W, Lamborg CH. Geochemistry of mercury in the environment. In: Lollar BS, Turekian KK. Environmental geochemistry, treatise on geochemistry. Oxford: Elsevier; 2007. 107–48.
8. US EPA. Minamata Convention on Mercury [Internet]. Washington (DC): United States Environmental Protection Agency; 2024 [cited 2024 Oct 4]. https://www.epa.gov/international-cooperation/minamata-convention-mercury
9. Bouse R, Fuller C, Luoma S, Hornberger M, Jaffe B, Smith R. Mercury-Contaminated Hydraulic Mining Debris in San Francisco Bay. SFEWS. 2010;8(1). https://doi.org/10.15447/sfews.2010v8iss1art3
10. Donovan PM, Blum JD, Yee D, Gehrke GE, Singer MB. An isotopic record of mercury in San Francisco Bay sediment. Chemical Geology. 2013;349–350:87–98. https://doi.org/10.1016/j.chemgeo.2013.04.017
11. Alpers CN, Hunerlach MP, May JT, Hothem RL. Mercury contamination from historical gold mining in California. US Geological Survey; 2005. 1–6.
12. James LA. Sediment from hydraulic mining detained by Englebright and small dams in the Yuba basin. Geomorphology. 2005;71(1–2):202–26. https://doi.org/10.1016/j.geomorph.2004.02.016
13. Ganguli PM, Mason RP, Abu-Saba KE, Anderson RS, Flegal AR. Mercury Speciation in Drainage from the New Idria Mercury Mine, California. Environ Sci Technol. 2000;34(22):4773–9. https://doi.org/10.1021/es991364y

14. Whyte DC, Kirchner JW. Assessing water quality impacts and cleanup effectiveness in streams dominated by episodic mercury discharges. Sci Total Environ. 2000;260(1–3):1–9. https://doi.org/10.1016/s0048-9697(00)00537-4 PMID: 11032111
15. Wiener JG, Suchanek TH. The basis for ecotoxicological concern in aquatic ecosystems contaminated by historical mercury mining. Ecol Appl. 2008;18(8 Suppl):A3-11. https://doi.org/10.1890/06-1939.1 PMID: 19475915
16. Jew AD, Kim CS, Rytuba JJ, Gustin MS, Brown GE Jr. New technique for quantification of elemental Hg in mine wastes and its implications for mercury evasion into the atmosphere. Environ Sci Technol. 2011;45(2):412–7. https://doi.org/10.1021/es1023527 PMID: 21121657
17. Marvin-DiPasquale M, Slotton D, Ackerman J, Downing-Kunz M, Jaffe B, Foxgrover A. South San Francisco Bay salt pond restoration project—A synthesis of phase-1 mercury studies. Menlo Park (CA): U.S. Geological Survey; 2023.
18. McKee L, Gilbraith A, Pearce S, Shimabuku I. Guadalupe river mercury concentrations and loads during the large rare January 2017 storm. Prepared for the Regional Monitoring Program for Water Quality in San Francisco Bay (RMP), Sources, Pathways and Loadings Workgroup. Contribution No. 837. Richmond (CA): San Francisco Estuary Institute; 2018.
19. Thomas MA, Conaway CH, Steding DJ, Marvin-DiPasquale M, Abu-Saba KE, Flegal AR. Mercury contamination from historic mining in water and sediment, Guadalupe River and San Francisco Bay, California. GEEA. 2002;2(3):211–7. https://doi.org/10.1144/1467-787302-024
20. Gehrke GE, Blum JD, Marvin-DiPasquale M. Sources of mercury to San Francisco Bay surface sediment as revealed by mercury stable isotopes. Geochimica et Cosmochimica Acta. 2011;75(3):691–705. https://doi.org/10.1016/j.gca.2010.11.012
21. Gehrke GE, Blum JD, Slotton DG, Greenfield BK. Mercury isotopes link mercury in San Francisco Bay forage fish to surface sediments. Environ Sci Technol. 2011;45(4):1264–70. https://doi.org/10.1021/es103053y PMID: 21250676
22. Kim CS, Brown GE Jr, Rytuba JJ. Characterization and speciation of mercury-bearing mine wastes using X-ray absorption spectroscopy. Sci Total Environ. 2000;261(1–3):157–68. https://doi.org/10.1016/s0048-9697(00)00640-9 PMID: 11036987
23. Kim CS, Rytuba JJ, Brown GE Jr. Geological and anthropogenic factors influencing mercury speciation in mine wastes: an EXAFS spectroscopy study. Applied Geochemistry. 2004;19(3):379–93. https://doi.org/10.1016/s0883-2927(03)00147-1
24. Lowry GV, Shaw S, Kim CS, Rytuba JJ, Brown GE Jr. Macroscopic and microscopic observations of particle-facilitated mercury transport from New Idria and Sulphur Bank mercury mine tailings. Environ Sci Technol. 2004;38(19):5101–11. https://doi.org/10.1021/es034636c PMID: 15506205
25. Rytuba JJ. Mercury mine drainage and processes that control its environmental impact. Sci Total Environ. 2000;260(1–3):57–71. https://doi.org/10.1016/s0048-9697(00)00541-6 PMID: 11032116
26. Rytuba JJ. Mercury from mineral deposits and potential environmental impact. Env Geol. 2003;43(3):326–38. https://doi.org/10.1007/s00254-002-0629-5
27. Rytuba JJ. Release of mercury mine tailings from mine-impacted watersheds by extreme events resulting from climate change. Presented at: AGU Fall Meeting. San Francisco, CA; 2015.
28. Wiederhold JG, Smith RS, Siebner H, Jew AD, Brown GE Jr, Bourdon B, et al. Mercury isotope signatures as tracers for Hg cycling at the New Idria Hg mine. Environ Sci Technol. 2013;47(12):6137–45. https://doi.org/10.1021/es305245z PMID: 23662941
29. Fitzgerald WF, Lamborg CH. Geochemistry of mercury in the environment. In: Lollar BS, Turekian KK, Environmental geochemistry, treatise on geochemistry. Oxford (UK): Elsevier; 2007. 107–48.
30. Driscoll CT, Mason RP, Chan HM, Jacob DJ, Pirrone N. Mercury as a global pollutant: sources, pathways, and effects. Environ Sci Technol. 2013;47(10):4967–83. https://doi.org/10.1021/es305071v PMID: 23590191
31. Gustin MS, Amos HM, Huang J, Miller MB, Heidecorn K. Measuring and modeling mercury in the atmosphere: a critical review. Atmos Chem Phys. 2015;15(10):5697–713. https://doi.org/10.5194/acp-15-5697-2015
32. Gworek B, Dmuchowski W, Baczewska-Dąbrowska AH. Mercury in the terrestrial environment: a review. Environ Sci Eur. 2020;32(1). https://doi.org/10.1186/s12302-020-00401-x
33. Bowman KP, Cohen PJ. Interhemispheric exchange by seasonal modulation of the hadley circulation. J Atmos Sci. 1997;54(16):2045–59.
34. Obrist D, Agnan Y, Jiskra M, Olson CL, Colegrove DP, Hueber J, et al. Tundra uptake of atmospheric elemental mercury drives Arctic mercury pollution. Nature. 2017;547(7662):201–4. https://doi.org/10.1038/nature22997 PMID: 28703199
35. Schuster PF, Schaefer KM, Aiken GR, Antweiler RC, Dewild JF, Gryziec JD, et al. Permafrost Stores a Globally Significant Amount of Mercury. Geophysical Research Letters. 2018;45(3):1463–71. https://doi.org/10.1002/2017gl075571
36. Kocman D, Wilson SJ, Amos HM, Telmer KH, Steenhuisen F, Sunderland EM, et al. Toward an Assessment of the Global Inventory of Present-Day Mercury Releases to Freshwater Environments. Int J Environ Res Public Health. 2017;14(2):138. https://doi.org/10.3390/ijerph14020138 PMID: 28157152
37. Obrist D, Kirk JL, Zhang L, Sunderland EM, Jiskra M, Selin NE. A review of global environmental mercury processes in response to human and natural perturbations: Changes of emissions, climate, and land use. Ambio. 2018;47(2):116–40. https://doi.org/10.1007/s13280-017-1004-9 PMID: 29388126
38. Ward DM, Nislow KH, Folt CL. Bioaccumulation syndrome: identifying factors that make some stream food webs prone to elevated mercury bioaccumulation. Ann N Y Acad Sci. 2010;1195:62–83. https://doi.org/10.1111/j.1749-6632.2010.05456.x PMID: 20536817
39. Cossaboon JM, Ganguli PM, Flegal AR. Mercury offloaded in Northern elephant seal hair affects coastal seawater surrounding rookery. Proc Natl Acad Sci U S A. 2015;112(39):12058–62. https://doi.org/10.1073/pnas.1506520112 PMID: 26372960

40. Morel FMM, Kraepiel AML, Amyot M. The chemical cycle and bioaccumulation of merCURY. Annu Rev Ecol Syst. 1998;29(1):543–66. https://doi.org/10.1146/annurev.ecolsys.29.1.543
41. Sunderland EM. Mercury exposure from domestic and imported estuarine and marine fish in the U.S. seafood market. Environ Health Perspect. 2007;115(2):235–42. https://doi.org/10.1289/ehp.9377 PMID: 17384771
42. Fujimura M, Usuki F. Cellular Conditions Responsible for Methylmercury-Mediated Neurotoxicity. Int J Mol Sci. 2022;23(13):7218. https://doi.org/10.3390/ijms23137218 PMID: 35806222
43. Aaseth J, Wallace DR, Vejrup K, Alexander J. Methylmercury and developmental neurotoxicity: A global concern. Current Opinion in Toxicology. 2020;19:80–7. https://doi.org/10.1016/j.cotox.2020.01.005
44. Bishop K, Shanley JB, Riscassi A, de Wit HA, Eklöf K, Meng B, et al. Recent advances in understanding and measurement of mercury in the environment: Terrestrial Hg cycling. Sci Total Environ. 2020;721:137647. https://doi.org/10.1016/j.scitotenv.2020.137647 PMID: 32197286
45. Seelen EA, Chen CY, Balcom PH, Buckman KL, Taylor VF, Mason RP. Historic contamination alters mercury sources and cycling in temperate estuaries relative to uncontaminated sites. Water Res. 2021;190:116684. https://doi.org/10.1016/j.watres.2020.116684 PMID: 33310435
46. Grigal DF. Inputs and outputs of mercury from terrestrial watersheds: a review. Environ Rev. 2002;10(1):1–39. https://doi.org/10.1139/a01-013
47. Seelen E, Liem-Nguyen V, Wünsch U, Baumann Z, Mason R, Skyllberg U, et al. Dissolved organic matter thiol concentrations determine methylmercury bioavailability across the terrestrial-marine aquatic continuum. Nat Commun. 2023;14(1):6728. https://doi.org/10.1038/s41467-023-42463-4 PMID: 37872168
48. DiMento BP, Mason RP. Factors controlling the photochemical degradation of methylmercury in coastal and oceanic waters. Mar Chem. 2017;196:116–25. https://doi.org/10.1016/j.marchem.2017.08.006 PMID: 29515285
49. Marvin-DiPasquale M, Agee J, McGowan C, Oremland RS, Thomas M, Krabbenhoft D, et al. Methyl-Mercury Degradation Pathways: A Comparison among Three Mercury-Impacted Ecosystems. Environ Sci Technol. 2000;34(23):4908–16. https://doi.org/10.1021/es0013125
50. Bull W. Geomorphology of segmented alluvial fans in western fresno county, california. Washington (DC): US Government Printing Office; 1964.
51. Cargill SM, Root DH, Bailey EH. Resource estimation from historical data: Mercury, a test case. Mathematical Geology. 1980;12(5):489–522. https://doi.org/10.1007/bf01028882
52. Coleman RG. Field trip guide book to New Idria area, California. Presented at: 14th General Meeting of the International Mineralogical Association. Stanford University: Stanford, CA; 1986. 40.
53. Boctor NZ, Shieh YN, Kullerud G. Mercury ores from the New Idria Mining District, California: Geochemical and stable isotope studies. Geochimica et Cosmochimica Acta. 1987;51(6):1705–15. https://doi.org/10.1016/0016-7037(87)90349-8
54. Studemeister PA. Mercury deposits of western California: an overview. Mineral Deposita. 1984;19(3). https://doi.org/10.1007/bf00199786
55. Rajakaruna N, Knudsen K, Fryday AM, O'Dell RE, Pope N, Olday FC, et al. Investigation of the importance of rock chemistry for saxicolous lichen communities of the New Idria serpentinite mass, San Benito County, California, USA. The Lichenologist. 2012;44(5):695–714. https://doi.org/10.1017/s0024282912000205
56. Laurs BM, Rohtert WR, Gray M. Benitoite from the New Idria District, San Benito County, California. Gems & Gemology. 1997;33(3):166–87. https://doi.org/10.5741/gems.33.3.166
57. Ramboll C. New idria data gaps analysis report. United States Environmental Protection Agency; 2019.
58. Nordstrom DK, Alpers CN. Geochemistry of acid mine waters. In: Plumlee GS, Logsdon MJ. The environmental geochemistry of mineral deposits. Washington (DC): Society of Economic Geologists; 1999. 133–60.
59. Presser TS. "The Kesterson effect". Environmental Management. 1994;18(3):437–54. https://doi.org/10.1007/bf02393872
60. California Department of Public Health (CA DPH). Public Health Assessment: Evaluation of exposure to contaminants at the New Idria Mercury Mine Superfund Site, San Benito, California. Atlanta (GA): Agency for Toxic Substances and Disease Registry; 2016. https://www.atsdr.cdc.gov/HAC/pha/NewIdriaMercuryMineSite/New_Idria_Mercury_Mine_PHA_7-7-2016_508.pdf
61. SWRCB. Final California 2020 Integrated Report (303(d) List/305(b) Report) – Supporting Information. California State Water Resources Control Board; 2022.
62. US EPA. In the Matter of: New Idria Mercury Mine Superfund Site San Benito County, California, Buckhom, Inc., Respondent. Administrative Settlement Agreement and Order on Consent for Remedial Investigation/Feasibility Study. Washington (DC): United States Environmental Protection Agency; 2018.
63. US EPA. New Idria Mercury Mine Site Profile [Internet]. Washington (DC): United States Environmental Protection Agency; 2023 [cited 2023 Sep 26]. https://cumulis.epa.gov/supercpad/cursites/csitinfo.cfm?id=0905346
64. US EPA. Water quality criterion for the protection of human health: Methylmercury. Washington (DC): United States Environmental Protection Agency; 2001.
65. RWQCB-CV. Methylmercury water quality objectives. In: The Water Quality Control Plan for the California Regional Water Quality Control Board Central Valley Region. Rancho Cordova (CA): California Regional Water Quality Control Board - Central Valley Region; 2019.
66. RWQCB-SFB. Marine water quality objectives for mercury in San Francisco Bay. In: Water Quality Control Plan for the San Francisco Bay Basin. Oakland (CA): California Water Resources Control Board; 2006.

67. Jackson A, Evers DC, Eagles-Smith CA, Ackerman JT, Willacker JJ, Elliott JE, et al. Mercury risk to avian piscivores across western United States and Canada. Sci Total Environ. 2016;568:685–96. https://doi.org/10.1016/j.scitotenv.2016.02.197 PMID: 26996522

68. Weston Solutions Inc. New Idria Mercury Mine Superfund Site, Idria, San Benito County, California, Removal Action Final Report. San Francisco (CA): United States Environmental Protection Agency, Region 9; 2012.

69. Cui X, Lamborg C, Hammerschmidt C, Xiang Y, Lam P. The effect of particle composition and concentration on the partitioning coefficient for mercury in three ocean basins. Front Environ Chem. 2021;2.

70. Kite G. Computerized streamflow measurement using slug injection. Hydrol Process. 1993;7(3):227–33.

71. Kite G. An extension to the salt dilution method of measuring streamflow. International Journal of Water Resources Development. 1989;5(1):19–24. https://doi.org/10.1080/07900628908722408

72. Ganguli PM. Mercury speciation in acid mine drainage: New Idria quicksilver mine, California. Santa Cruz (CA): University of California, Santa Cruz; 1998.

73. Santofimia E, González-Toril E, López-Pamo E, Gomariz M, Amils R, Aguilera A. Microbial Diversity and Its Relationship to Physicochemical Characteristics of the Water in Two Extreme Acidic Pit Lakes from the Iberian Pyrite Belt (SW Spain). PLoS One. 2013;8(6):e66746. https://doi.org/10.1371/journal.pone.0066746 PMID: 23840525

74. Kotalik CJ, Cadmus P, Clements WH. Indirect Effects of Iron Oxide on Stream Benthic Communities: Capturing Ecological Complexity with Controlled Mesocosm Experiments. Environ Sci Technol. 2019;53(19):11532–40. https://doi.org/10.1021/acs.est.9b04236 PMID: 31483623

75. Branfireun BA, Roulet NT, Kelly CarolA, Rudd JWM. In situ sulphate stimulation of mercury methylation in a boreal peatland: Toward a link between acid rain and methylmercury contamination in remote environments. Global Biogeochemical Cycles. 1999;13(3):743–50. https://doi.org/10.1029/1999gb900033

76. Gilmour CC, Henry EA, Mitchell R. Sulfate stimulation of mercury methylation in freshwater sediments. Environ Sci Technol. 1992;26(11):2281–7. https://doi.org/10.1021/es00035a029

77. Gilmour CC, Riedel GS, Ederington MC, Bell JT, Gill GA, Stordal MC. Biogeochemistry. 1998;40(2/3):327–45. https://doi.org/10.1023/a:1005972708616

78. Orem WH, Krabbenhoft DP, Poulin BA, Aiken GR. Sulfur contamination in the Everglades, a major control on mercury methylation. In: Rumbold DG, Pollman CD, Axelrad DM. Mercury and the Everglades. Cham (Switzerland): Springer International Publishing; 2019. 13–48. https://doi.org/10.1007/978-3-030-32057-7_2

79. Capo E, Cosio C, Gascón Díez E, Loizeau J-L, Mendes E, Adatte T, et al. Anaerobic mercury methylators inhabit sinking particles of oxic water columns. Water Res. 2023;229:119368. https://doi.org/10.1016/j.watres.2022.119368 PMID: 36459894

80. Ortiz VL, Mason RP, Ward JE. An examination of the factors influencing mercury and methylmercury particulate distributions, methylation and demethylation rates in laboratory-generated marine snow. Mar Chem. 2015;177(Pt 5):753–62. https://doi.org/10.1016/j.marchem.2015.07.006 PMID: 26644635

81. Walch H, von der Kammer F, Hofmann T. Freshwater suspended particulate matter-Key components and processes in floc formation and dynamics. Water Res. 2022;220:118655. https://doi.org/10.1016/j.watres.2022.118655 PMID: 35665676

82. Hinkle SR, Bencala KE, Wentz DA, Krabbenhoft DP. Mercury and Methylmercury Dynamics in the Hyporheic Zone of an Oregon Stream. Water Air Soil Pollut. 2013;225(1). https://doi.org/10.1007/s11270-013-1694-y

83. Regnell O, Watras CJ. Microbial Mercury Methylation in Aquatic Environments: A Critical Review of Published Field and Laboratory Studies. Environ Sci Technol. 2019;53(1):4–19. https://doi.org/10.1021/acs.est.8b02709 PMID: 30525497

84. Hu H, Lin H, Zheng W, Tomanicek SJ, Johs A, Feng X, et al. Oxidation and methylation of dissolved elemental mercury by anaerobic bacteria. Nature Geosci. 2013;6(9):751–4. https://doi.org/10.1038/ngeo1894

85. Krabbenhoft DP, Wiener JG, Brumbaugh WG, Olson ML, DeWild JF, Sabin TJ. A national pilot study of mercury contamination of aquatic ecosystems along multiple gradients. U.S. Geological Survey Toxic Substances Hydrology Program: Contamination of hydrologic systems and related ecosystems. Washington (DC): US Geological Survey; 1999.

86. Barkay T, Gu B. Demethylation-The Other Side of the Mercury Methylation Coin: A Critical Review. ACS Environ Au. 2022;2(2):77–97. https://doi.org/10.1021/acsenvironau.1c00022 PMID: 37101582

87. Levick L, Goodrich D, Hernandez M, Fonseca J, Semmens D, Stromber J, et al. The ecological and hydrological significance of ephemeral and intermittent streams in the arid and semi-arid American Southwest. Southwest Watershed Res Cent. 2008;116.

88. Rivers JW, Johnson JM, Haig SM, Schwarz C, Burnett LJ, Brandt J, et al. An analysis of monthly home range size in the critically endangered California CondorGymnogyps californianus. Bird Conservation International. 2014;24(4):492–504. https://doi.org/10.1017/s0959270913000592

89. Herring G, Eagles-Smith CA, Varland DE. Mercury and lead exposure in avian scavengers from the Pacific Northwest suggest risks to California condors: Implications for reintroduction and recovery. Environ Pollut. 2018;243(Pt A):610–9. https://doi.org/10.1016/j.envpol.2018.09.005 PMID: 30218871

90. Bocharova N, Treu G, Czirják GÁ, Krone O, Stefanski V, Wibbelt G, et al. Correlates between feeding ecology and mercury levels in historical and modern arctic foxes (Vulpes lagopus). PLoS One. 2013;8(5):e60879. https://doi.org/10.1371/journal.pone.0060879 PMID: 23671561

91. Huang X, Swain DL. Climate change is increasing the risk of a California megaflood. Sci Adv. 2022;8(32):eabq0995. https://doi.org/10.1126/sciadv.abq0995 PMID: 35960799

92. Sharma RK, Weinman B. Geochemical evidence of chemical and physical weathering of mine waste downriver from the New Idria Mercury Mine, San Benito County, California. Presented at: AGU Fall Meeting. San Francisco, CA. 2014.

93. Grenier L, Melwan A, Hunt J, Bezalel S, Davis J, Ichikawa G, et al. California Bay-Delta Authority Fish Mercury Project Year 1 Annual Report: Sport fish sampling and analysis. Richmond (CA): San Francisco Estuary Institute; 2007.